Draft version April 22, 2016
Preprint typeset using LaTeX style emulateapj v. 5/2/11

arXiv:1604.06399v1 [astro-ph.SR] 21 Apr 2016

ORBITS OF SUBSYSTEMS IN FOUR HIERARCHICAL MULTIPLE STARS.

Andrei Tokovinin
Cerro Tololo Inter-American Observatory, Casilla 603, La Serena, Chile
Draft version April 22, 2016

ABSTRACT

Seven spectroscopic orbits in nearby solar-type multiple stars are presented. The primary of the chromospherically active star HIP 9642 is a 4.8-day double-lined pair; the outer 420-yr visual orbit is updated, but remains poorly constrained. HIP 12780 is a quadruple system consisting of the resolved 6.7-yr pair FIN 379 Aa,Ab, for which the combined orbit, masses, and orbital parallax are determined here, and the single-lined binary Ba,Bb with a period of 27.8 days. HIP 28790 is a young quintuple system composed of two close binaries Aa,Ab and Ba,Bb with periods of 221 and 13 days, respectively, and a single distant component C. Its subsystem Ba,Bb is peculiar, having the spectroscopic mass ratio of 0.89 but a magnitude difference of ∼2.2 mag. HIP 64478 also contains five stars: the A-component is a 29-year visual pair with a previously known 4-day twin subsystem, while the B-component is a contact binary with a period of 5.8 hours, seen nearly pole-on.

Subject headings: stars: binaries

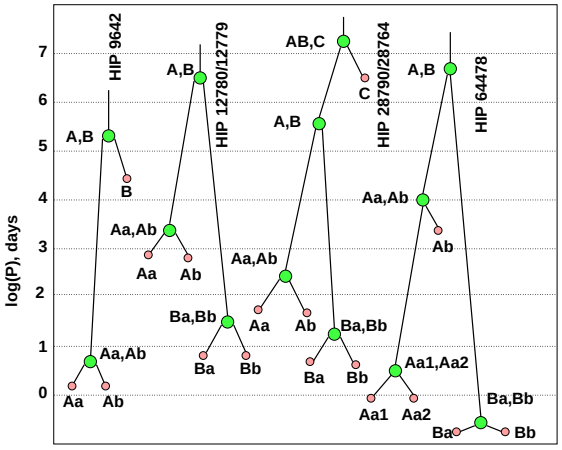

Figure 1. Structure of four hierarchical multiple systems. Larger green circles depict subsystems (nodes), smaller pink circles are individual stars. Vertical position of the nodes reflects orbital periods on a logarithmic scale.

1. INTRODUCTION

Radial velocities (RVs) of nearby solar-type multiple systems were monitored in 2014 and 2015 to determine the frequency of spectroscopic subsystems in visually resolved components and to follow their orbital motion. The resulting statistics were reported by Tokovinin (2015), while detailed analysis of individual systems was deferred to future publications. Four triple-lined multiples were featured in Paper I (Tokovinin 2016), and this is the second paper in this series. About a dozen of remaining stars with variable RVs observed in this survey mostly have long orbital periods and still lack sufficient data for computing their orbits.

Identifications and basic data on the four multiple systems studied here are given in Table 1. They have solar-type primary components and are located within 50 pc of the Sun. The proper motions (PMs) and parallaxes are from van Leeuwen (2007), hereafter HIP2. The spectral types, V magnitudes, and $B-V$ colors are taken from SIMBAD. Galactic velocities U, V, W in the last three columns are computed using the HIP2 astrometry and the center-of-mass RVs determined here (the U axis points away from the Galactic center). The following common abbreviations are used throughout this paper: SB1 and SB2 — single - and double-lined spectroscopic binaries, AO — adaptive optics, PM — proper motion. As in Paper I, components of multiple systems are designated by single letters or strings, subsystems are denoted by their two components joined with a comma. Figure 1 depicts the hierarchical structure of objects featured here: one triple, one quadruple, and two quintuple systems.

The observational material and data analysis are briefly presented in Section 2, main results are tabulated in Section 3. Sections 4 to 7 are devoted to the individual systems. The paper is summarized in Section 8.

2. OBSERVATIONS AND DATA ANALYSIS

The observational material used here and the data reduction methods are covered in Tokovinin (2015) and in Paper I. They are recalled here briefly. Most spectra were taken with the 1.5-m telescope located at the Cerro Tololo Interamerican Observatory in Chile and operated by the SMARTS Consortium.[1] The observing time was allocated through NOAO (programs 14B-0009, 15A-0055, 15B-0012). The observations were made with the CHIRON fiber-fed echelle spectrograph (Tokovinin et al. 2013) by the telescope operators in the service mode. HIP 64478 was observed in the fiber mode with a spectral resolution of $R = 28,000$, all other stars were observed in the slicer mode with $R = 80,000$. A few spectra taken in 2010 at the same telescope with the Fiber Echelle (FECH) with a resolution of $R = 44,000$ are used, as well as the RVs measured with the echelle spectrometer at the Du Pont 2.5-m telescope (Tokovinin et al. 2015a).

The RVs were derived from the cross-correlation function (CCF) of the spectrum with a binary mask in the spectral range from 4500Å to 6500Å. The CCF is ap-

atokovinin@ctio.noao.edu

[1] http://www.astro.yale.edu/smarts/

Table 1
Basic parameters of multiple systems

HIP	HD	WDS (J2000)	Spectral type	V (mag)	$B-V$ (mag)	μ_α^* (mas yr^{-1})	μ_δ	$\pi_{\rm HIP2}$[a] (mas)	U	V (km s^{-1})	W
9642	12759	02039−4525	G5V	7.31	0.69	+328	+52	20.44 ± 0.55	−63.4	−59.8	−27.4
12780	17134	02442−2530	G3V	6.96	0.63	+166	+51	24.20 ± 1.16	−27.1	−14.1	14.8
12779	...	02442−2530	K0V?	9.05	0.84	+165	+52	22.86 ± 1.21	...	...	...
28790	41742	06047−4505	F4V	5.93	0.49	−79	+255	37.18 ± 0.64	−39.2	−11.0	−14.4
28764	41700	06047−4505	F8V	6.35	0.52	−81	+246	37.64 ± 0.25	...	...	...
64478	114630	13129−5949	G0V	6.22	0.59	+7	−108	23.72 ± 0.60	11.1	−16.1	−20.7

[a] Proper motions and parallax from HIP2 (van Leeuwen 2007).

Table 2
CCF parameters and V magnitudes

HIP	Comp.	a	σ (km s^{-1})	$a\sigma$ (km s^{-1})	V (mag)
9642	Aa	0.262	4.49	1.174	7.70
9642	Ab	0.118	4.10	0.482	8.66
12780	Aa	0.237	3.52	0.835	7.56
12780	Ab	0.172	3.60	0.621	7.88
12780	Ba	0.429	3.30	1.570	9.05
28790	Aa	0.072	14.84	1.071	6.02
28790	Ba	0.337	4.52	1.510	9.11
28790	Bb	0.051	3.93	0.197	11.32
64478	Aa1	0.067	10.19	0.681	6.99
64478	Aa2	0.068	10.20	0.689	6.99
64478	Ab	0.011	5.72	0.065	10.65
64478	Ba	0.052	24.80	1.277	9.97
64478	Bb	0.043	19.53	0.851	10.42

proximated by one or several Gaussian functions; their centers give the RVs (after applying the barycentric correction), while the amplitudes a and dispersions σ characterize the depth and width of the spectral lines. Paper I gives approximate relation between σ and the projected rotational velocity $V \sin i$.

The orbital elements and their errors were determined by the least-squares fit to the RVs with weights inversely proportional to the adopted errors. The IDL code `orbit`[2] was used. It can fit spectroscopic, visual, or combined visual/spectroscopic orbits. Formal errors of orbital elements are determined from these fits. For combined orbits, the errors of orbital masses and parallax are computed by taking into account correlations between individual elements. Masses of the stars that are not derived directly from the orbits, as well as other parameters, are estimated from the absolute magnitudes using standard relations for main-sequence stars (see Paper I).

3. MAIN RESULTS

Table 2 contains average parameters of the CCFs (unresolved CCFs from blended spectra are not used in the averaging). The last column lists individual V-band magnitudes of the components computed from the spectroscopic flux ratios (assumed to be proportional to $a\sigma$) and the combined magnitudes. These estimates are accurate to ∼0.1 mag and would not be compromised by undetected small-amplitude photometric variability.

Spectroscopic orbital elements derived in this work are listed in Table 3, in common notation. Its first two columns contain the *Hipparcos* number of the primary component and the subsystem designation. Then follow the orbital period P, time of periastron T (for circular orbits it corresponds to the RV maximum), eccentricity e, longitude of periastron of the primary component $\omega_{\rm A}$, RV amplitudes K_1 and K_2 of the primary and secondary components, respectively, and the center-of-mass velocity γ. The last column gives the weighted rms residuals for both components. The visual orbits are assembled in Table 4 (a — semi-major axis, $\Omega_{\rm A}$ — position angle of the node, $\omega_{\rm A}$ — longitude of periastron, i — inclination). The combined orbit of HIP 12780 Aa,Ab is featured in both tables, duplicating the overlapping elements. In the combined orbit, the longitude of periastron $\omega_{\rm A}$ corresponds to the primary, and the position angle of the visual orbit $\Omega_{\rm A}$ is chosen accordingly to describe the motion of the secondary.

The observations used in orbit calculations are listed in two tables, published in full electronically. Table 5 gives, for each date, the RVs of the primary and secondary components V_1 and V_2, their errors used for relative weighting (unrealistically large errors are assigned to RVs corresponding to blended CCFs), and residuals to the orbit O−C. The first column contains the *Hipparcos* number, the second column identifies the system. The dates are given in Julian days (minus 2,400,000). The last column of Table 5 specifies the data source. The resolved measurements are listed in Table 6 in a similar way as the RVs, with the first two columns identifying the system. Then follow the date in Besselian years, position angle θ, separation ρ, position error σ_ρ, residuals to orbit, and reference.

The following Sections discuss each multiple system individually.

4. HIP 9642

This star is a visual binary RST 2272. Its preliminary visual orbit by Hartkopf & Mason (2011), revised here, has $P = 549.83$ yr and a=3.″233, leading to the unrealistically large mass sum of 13 $\mathcal{M}_\odot$. The visual secondary B is much fainter than A ($\Delta Hp = 4.21$, $\Delta y = 4.89$, $\Delta I \sim 4.4$ mag), contributing little light to the combined spectrum. Its separation was last measured in 2015 at 1.″5, so the light of B is further attenuated by the 2.″7 entrance aperture of the spectrograph. It has no detectable signature in the CCFs.

The star is a bright X-ray source and it has an extremely high chromospheric activity (Makarov 2003). The spectroscopic subsystem Aa,Ab was discovered by Nordström et al. (2004). These authors estimated the mass ratio of 0.86 from nine observations, but did not determine the orbit. Two observations reported by Tokovinin et al. (2015a) show a substantial RV variation

[2] `http://www.ctio.noao.edu/~{}atokovin/orbit/`

Table 3
Spectroscopic orbits

HIP	System	P (d)	T (JD −2 400 000)	e	ω_A (deg)	K_1 (km s^{-1})	K_2 (km s^{-1})	γ (km s^{-1})	rms$_{1,2}$ (km s^{-1})
9642	Aa,Ab	4.78149	56970.0145	0	0	27.591	31.201	49.051	0.13
		± 0.00002	±0.0018	fixed	fixed	±0.092	±0.092	±0.04	0.12
12780	Aa,Ab	2443.1	54775.59	0.4999	191.20	7.440	8.050	−0.490	0.09
		±2.1	±2.5	±0.0015	±0.59	±0.041	±0.041	±0.040	0.10
12780	Ba,Bb	27.7679	56999.062	0.274	82.78	19.462	...	−0.322	0.01
		±0.0033	±0.077	±0.007	±1.23	±0.129	...	±0.066	...
28790	Aa,Ab	221.385	57013.906	0.833	195.99	21.128	...	26.250	0.04
		±0.014	±0.218	±0.010	±0.46	±1.63	...	±0.081	...
28790	Ba,Bb	13.2309	57004.908	0.231	123.7	21.513	24.151	28.376	0.27
		±0.0003	±0.118	±0.017	±3.4	±0.596	±0.448	±0.218	0.39
64478	Aa1,Aa1	4.2334536	57120.507	0	0	85.172	85.364	15.364	0.22
		±0.0000018	±0.004	fixed	fixed	± 0.40	± 0.40	±0.237	0.18
64478	Ba,Bb	0.243524	57119.4786	0	0	29.545	63.076	19.589	0.53
		±0.000003	±0.0004	fixed	fixed	±0.182	±0.637	±0.160	1.83

Table 4
Visual orbits

HIP	System	P (yr)	T (yr)	e	a (arcsec)	Ω_A (deg)	ω_A (deg)	i (deg)
9642	A,B	415.0	2327.57	0.2645	1.659	301.3	175.5	36.0
12780	Aa,Ab	6.68917	2008.846	0.4999	0.1002	183.77	191.20	42.00
		±0.0051	±0.007	±0.0015	± 0.0006	±0.49	±0.59	±0.72
64478	Aa,Ab	29.11	1997.27	0.173	0.3134	279.7	326.4	89.0
		±0.34	±1.55	±0.018	±0.0034	±0.2	±17.6	±0.4

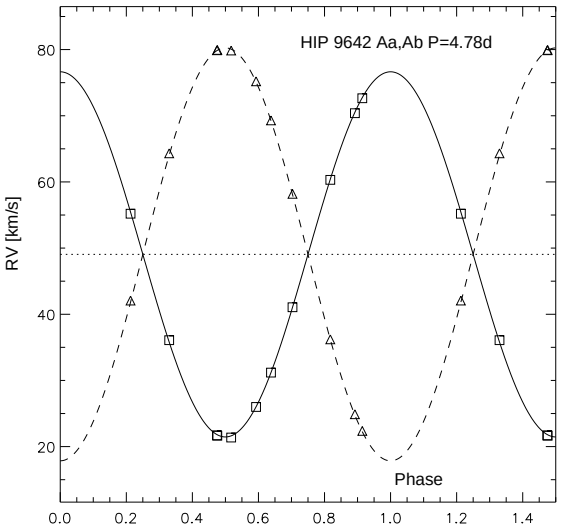

Figure 2. Orbit of HIP 9642 Aa,Ab with $P = 4.78$ d. In this and following plots, RVs of the primary and secondary components are plotted as squares and triangles, respectively, while their RV curves are traced by the full and dashed lines. The horizontal dotted line indicates the γ-velocity.

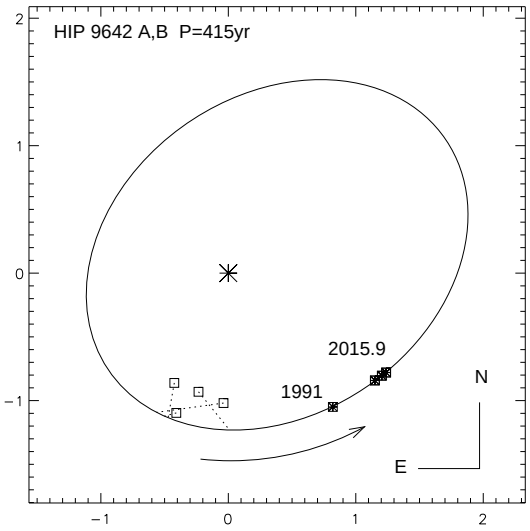

Figure 3. New visual orbit of HIP 9642 A,B (RST 2272) with $P = 415$yr. Positions of the secondary component B relative to the primary A at coordinate origin are plotted as squares (empty symbols for visual data, filled symbols for speckle data). They are connected by dotted lines to the calculated positions on the orbital ellipse. The scale of the axes is in arcseconds.

in one day, hinting at short period. The monitoring with CHIRON leads to a circular orbit of Aa,Ab with a period of 4.78 days (Figure 2). The eccentricity and longitude of periastron were fixed at zero in the orbit adjustment.

Using the HIP2 parallax, the magnitudes of Aa and Ab, and the Dartmouth isochrone for solar metallicity (Dotter et al. 2008), I estimated the masses of Aa and Ab at 1.12 and 0.94 $\mathcal{M}_\odot$. The spectroscopic orbit leads to $M_1 \sin^3 i$ of 0.05 $\mathcal{M}_\odot$. Therefore, the inclination of the spectroscopic pair is small, about 22°. The mass of B is estimated at 0.56 $\mathcal{M}_\odot$ (a late-K dwarf), the system mass sum is 2.62 $\mathcal{M}_\odot$. However, the system model based on the isochrones predicts the $V - K_s$ and $B - V$ colors of 1.39 and 0.53 mag, respectively, while the actual color indices are 1.78 and 0.69 mag. So, the stars are redder than normal main-sequence dwarfs (possibly evolved), and the estimates of their masses may be inaccurate. The semi-major axis of Aa,Ab is 1.5 mas, so the inner pair can be resolved by long-baseline interferometers.

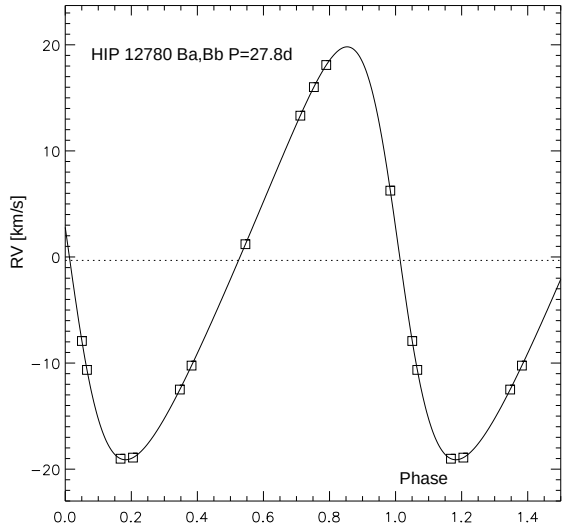

Figure 4. Spectroscopic orbit of HIP 12780 Ba,Bb with P = 27.8 d.

The visual orbit of the outer system A,B lacks coverage. Figure 3 illustrates an alternative orbit that corresponds to the mass sum of 3.10 $\mathcal{M}_\odot$, using the HIP2 parallax. It was obtained by weighting speckle data more strongly, in agreement with their realistic errors, and by fixing some elements. The visual orbit remains provisional (for this reason no errors are listed in Table 4), but the new elements are preferable because they will give a more accurate ephemeris in the near term. The inclination of the outer orbit, 36°, if trustworthy, differs from the estimated inclination of 22° in the inner orbit.

The kinematics (Table 1) and the absence of the 6708Å lithium line suggest that this multiple system is not very young. Its high chromospheric activity likely results from the tidal coupling of stellar rotation and orbit.

5. HIP 12780

The primary component HIP 12780 is a bright visual binary FIN 379 Aa,Ab with a known 6.7-yr orbit (Hartkopf et al. 2012). The tertiary component B = HIP 12779 is located at 12.″5 from A. The two stars have common parallax and PM. However, the first RV measurement with CHIRON have demonstrated that RV(B) differs substantially from RV(A). Further monitoring revealed that B is an SB1. Therefore, this multiple system is a 2+2 quadruple.

The spectroscopic orbit of Ba,Bb with P = 27.8 d is shown in Figure 4. The very small rms residuals of 6 m s^{-1} are partially explained by the fact that six orbital elements are derived from only 11 RV measurements. The estimated mass of Ba, 0.87 $\mathcal{M}_\odot$, corresponds to the minimum mass of 0.25 $\mathcal{M}_\odot$ for Bb. It is natural that Bb is not detected in the CCF. The component B was observed with speckle interferometry at SOAR and unresolved.

The visual orbit of the main pair Aa,Ab has been recently revised by Hartkopf et al. (2012). It is in excellent agreement with the RVs of Aa and Ab deduced from double CCFs. Adding recent data from speckle interferometry at SOAR (Tokovinin et al. 2015b), I computed the combined orbit depicted in Figure 5. The weighted

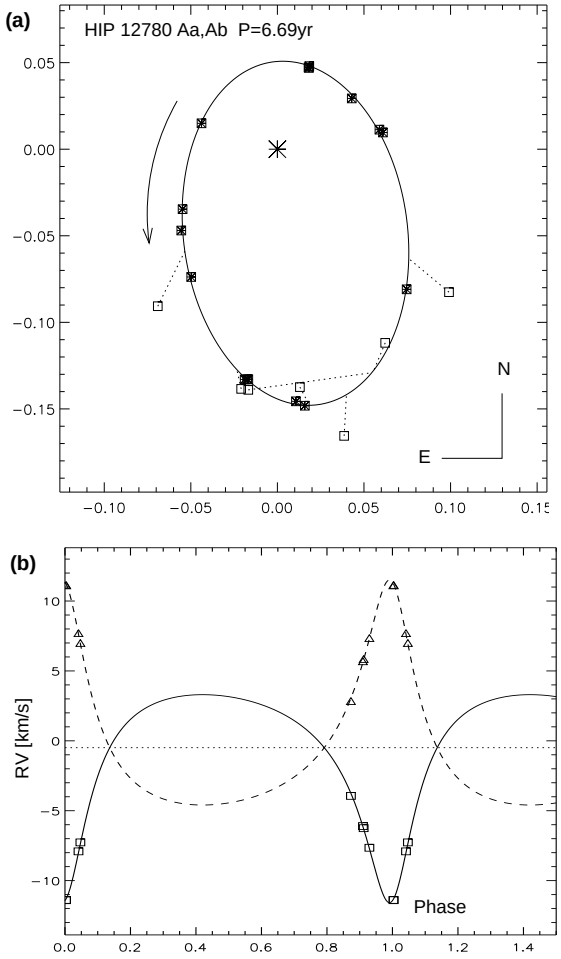

Figure 5. Combined orbit of HIP 12780 Aa,Ab = FIN 379. Top (a): orbit in the sky, bottom (b): the RV curve.

rms deviations are 1.°2 in angle, 1.2 mas in separation, and 92 and 96 m s^{-1} for the RVs of Aa and Ab, respectively. The combined orbit leads to the masses of 1.05±0.05 and 0.98±0.04 $\mathcal{M}_\odot$ for Aa and Ab and the orbital parallax is 22.26±0.40 mas. Note that the parallax of B = HIP 12779 is 22.9±1.2 mas, close to the orbital parallax of Aa,Ab. The *Hipparcos* parallax of the main star A, 24.2 mas, could be slightly biased by its fast orbital motion. The γ-velocities of A and B differ by only 0.17 km s^{-1}.

The spectroscopic magnitude difference of Aa,Ab deduced from the areas of the CCF dips is 0.32 mag. The five speckle measures lead to the mean Δy = 0.37 mag, with rms scatter of 0.09 mag. Adopting the spectroscopic ΔV and the orbital parallax, the Dartmouth isochrones (Dotter et al. 2008) lead to the masses that are 5% larger than the actually measured ones. On the other hand, the combined colors of the component A deduced from the *measured* masses and the isochrones are in excellent agreement with the actual colors. The 6708Å lithium line is not detectable in the spectra of Aa, Ab, and Ba.

6. HIP 28790

HIP 28790 is a young quintuple stellar system. The 5.″9 pair HJ 3834 A,B (V = 6.02; 8.98) is accompanied by the bright (V = 6.39) component C = HIP 28764 at a distance of 196″. Both A and B are spectroscopic binaries.

Table 5
Radial velocities and residuals (fragment)

HIP	System	Date (JD −2400000)	V_1	σ_1 (km s^{-1})	(O−C)$_1$	V_2	σ_2 (km s^{-1})	(O−C)$_2$	Ref.[a]
9642	Aa,Ab	54781.6711	36.080	0.500	0.290	64.320	0.500	0.273	L
9642	Aa,Ab	54782.5680	21.370	0.500	−0.254	79.860	0.500	−0.206	L
9642	Aa,Ab	56896.8724	41.060	0.200	0.029	58.201	0.200	0.080	C
9642	Aa,Ab	56938.8177	21.646	0.200	−0.140	79.949	0.200	0.066	C
12780	Aa,Ab	55446.0506	0.235	10.000	−2.410	...	...	...	F
12780	Aa,Ab	56908.8456	−3.938	0.050	−0.161	2.846	0.050	−0.179	C

[a] C: CHIRON; F: FECH; S: Saar et al. (1990); H: HARPS; L: Tokovinin (2015).

Table 6
Position measurements and residuals (fragment)

HIP	System	Date (yr)	θ (°)	ρ ($''$)	σ ($''$)	(O−C)$_\theta$ (°)	(O−C)$_\rho$ ($''$)	Ref.[a]
9642	A,B	1932.9100	177.9	1.020	0.500	34.9	−0.196	Vis
9642	A,B	1991.2500	218.0	1.332	0.010	1.6	0.030	HIP
9642	A,B	2008.7700	233.9	1.427	0.002	−0.1	−0.004	SOAR
12780	Aa,Ab	1963.0500	142.7	0.1140	1.0500	3.5	0.0324	Fin
12780	Aa,Ab	1991.7240	186.1	0.1490	0.0020	0.2	0.0006	Spe
12780	Aa,Ab	2015.0280	304.4	0.0520	0.0020	−1.3	−0.0014	SOAR

[a] Fin: ocular interferometry by W. S. Finsen; HIP: Hipparcos; SOAR: speckle interferometry at SOAR; Spe: speckle interferometry at other telescopes; Vis: visual micrometer measures.

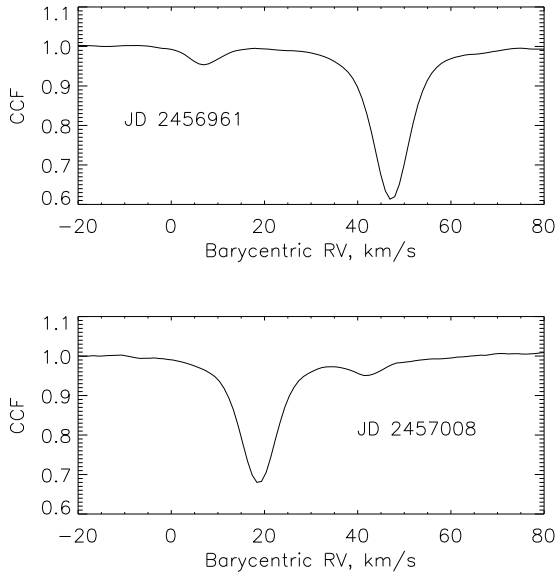

Figure 6. CCFs of HIP 28790B on two dates showing double profile are plotted on the same scale. Note variable amplitude of the main dip, 0.37 and 0.30 respectively.

The RV variation of A was discovered by Lagrange et al. (2009), the binarity of B was found by Tokovinin et al. (2015a), see Figure 6. Spectroscopic orbits of both subsystems are determined here.

Common PM, parallax, and RV establish the physical nature of the wide pair AB,C. The orbital periods of AB,C and A,B estimated from projected separations are 180 kyr and 1 kyr, respectively. The binary A,B was observed with AO by two groups (Tokovinin et al. 2010; Eirenreich et al. 2010) and no additional resolved components were found. The component B was also unresolved by speckle interferometry at SOAR. According to the Washington Double-Star Catalog, WDS (Mason et al. 2001), the pair A,B was at $1\farcs1$, 246° when it was discovered in 1837 and opened up to $5\farcs9$, 215° in 2010.

The component A has a fast axial rotation: the width of its CCF dip corresponds to $V \sin i = 26.0$ km s^{-1} according to the formula of Paper I. Ammler-von & Reiners (2012) measured $V \sin i = 26.7$ km s^{-1} and $T_e = 6324$ K. Gray et al. (2006) determined spectral types of F5.5V, K4.5V, and F9V for A, B, and C, respectively, and estimated effective temperatures of A and C at 6446 K and 6241 K. They found that C is chromospherically active. This has been established earlier by Cutispoto et al. (2002), who measured the rotation of C as $V \sin i = 16.2$ km s^{-1}. Mannings & Barlow (1998) detected thermal emission from dust and identified the main star as "Vega-like". Kalas et al. (2002) mentioned that the system belongs to the β Pictoris group, but its spatial velocity (Table 1) does not support this claim; instead, it is close to that of the Hyades cluster. The spectrum of the component A contains the line of lithium at 6708Å (it is broadened by fast rotation and difficult to measure), while no such line is present in the spectrum of B.

Figure 7 (top) shows the orbital solution for the subsystem Aa,Ab. RVs from CHIRON are used together with the RVs measured by Lagrange et al. (2009) with HARPS. These authors have kindly provided individual RVs, not given in the paper, on my request. However, they measured RVs relative to the mean velocity. An offset of +29.62 km s^{-1} was found iteratively to place those HARPS RVs on the absolute scale. The two data sets together cover well the descending branch of the RV curve in this eccentric ($e = 0.83$) orbit, with rms residuals of only 39 m s^{-1} despite fast stellar rotation. More observations should be planned to cover the periastron. If the mass of Aa is 1.2 $\mathcal{M}_\odot$, the minimum mass of Ab is 0.47 $\mathcal{M}_\odot$.

The component B is an SB2. The RV of the main CCF dip is variable, and sometimes there is a weak detail moving in anti-phase with the main dip. Figure 6 shows

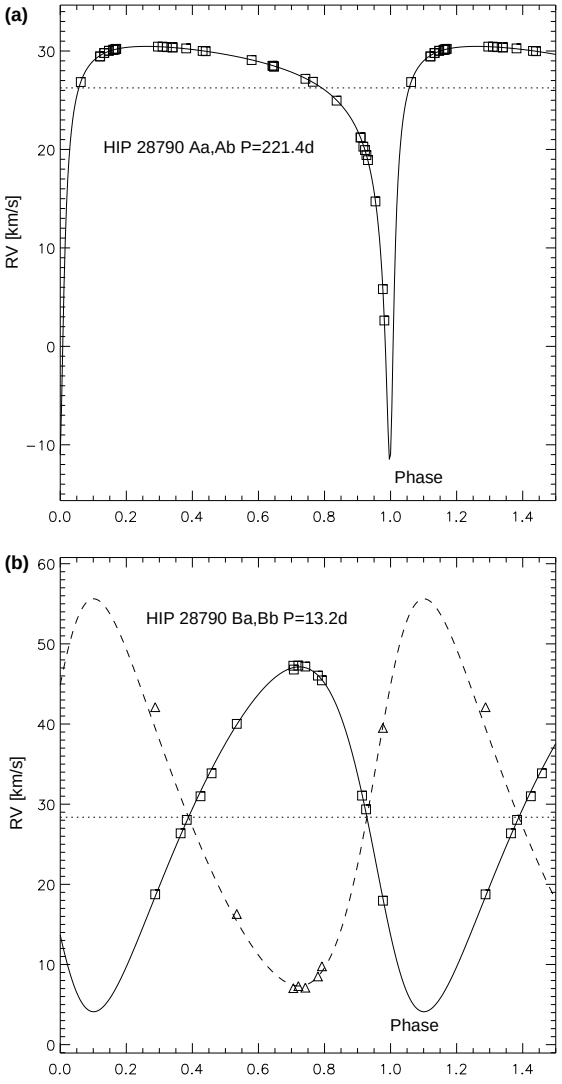

Figure 7. Top (a): the spectroscopic orbit of HIP 28790 Aa,Ab, $P = 221.4$d. Bottom (b): the RV curve of HIP 28790 Ba,Bb, $P = 13.23$ d.

examples of such CCFs. The SB2 orbit with $P = 13.2$ d is illustrated in the bottom plot of Figure 7. Approximation of the CCF by two Gaussians is not very good, the fit fails in some cases without fixing the width of the secondary dip. The rms residuals to the orbit are larger than usual. The variability of the CCF amplitude is caused by contamination by the light of the component A, three magnitudes brighter than B and only at 5.″9 distance. The entrance aperture of CHIRON has a diameter of 2.″7. Depending on the position of B on the aperture (while guiding on the component A) and on the seeing, a variable fraction of the light from A enters the aperture and dilutes the spectrum of B. The CCFs of strongly contaminated spectra contain a wide and weak dip corresponding to the A-component.

The RV amplitudes of Ba,Bb indicate a mass ratio $q = 0.89$, but the CCF dips are very unequal: the ratio of their areas corresponds to $\Delta V \approx 2.2$ mag. The component Bb must have a somewhat later spectral type than Ba, contributing to the smaller area of its CCF dip. Still, the substantial difference of the CCF areas of Ba and Bb has no explanation.

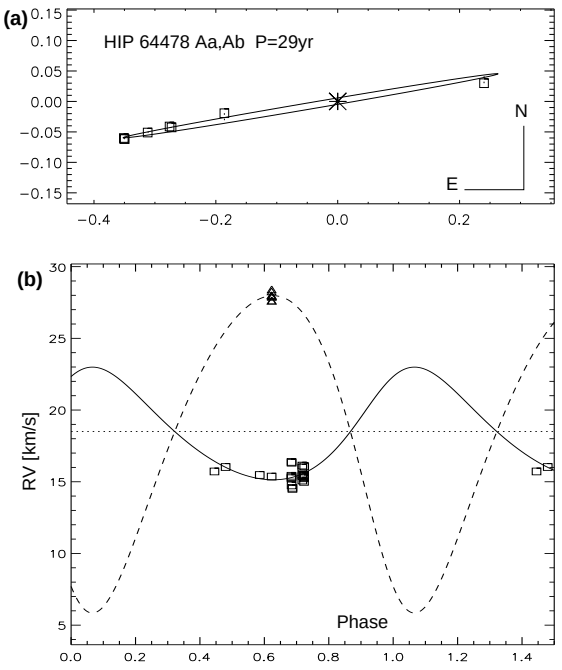

Figure 8. Orbit of HIP 64478 Aa,Ab = HDS 1850, $P = 29$ yr. Top (a): orbit in the plane of the sky, bottom (b): the RV curve.

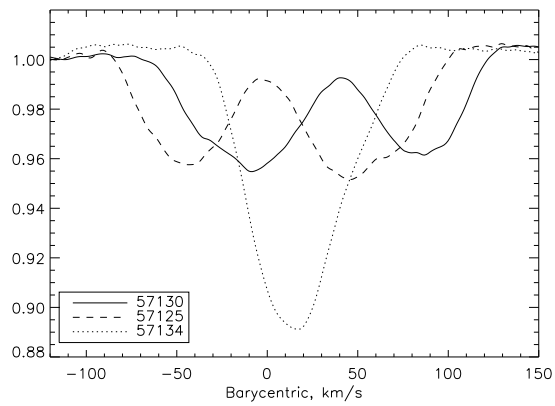

Figure 9. CCFs of HIP 64478B on three representative dates.

The γ-velocities of A and B are 26.25 and 28.38 km s^{-1}, respectively, while the RV of C is 27.4 km s^{-1} and constant according to Nordström et al. (2004). The wide pair AB,C is certainly physical, while the small RV difference between A and B is explained by the orbital motion of A,B. The agreement of RVs makes it unlikely that this system contains undiscovered close components, unless they have a very low mass or a highly inclined orbit. The component C was observed with the speckle camera at SOAR and unresolved.

7. HIP 64478

The quintuple system HIP 64478 is also known as HR 4980 or HD 114630. When Saar et al. (1990) determined the 4.2-day SB2 orbit of this chromospherically active G0V binary, its close visual companion had not yet been discovered by *Hipparcos*, while the companion B located at 25″ and 146° from A appeared irrelevant. Those authors wrongly denoted the spectroscopic com-

ponents as A and B, while WDS had not yet assigned any designation for B and denoted the visual pair as COO 152. The outer system A,B is definitely physical, keeping the same position since its discovery in 1892; its period estimated from projected separation is about 17 kyr. The PM of B is $(+1, -97)$ mas yr^{-1}, its photometry: $V = 9.42$, $K_s = 6.68$ mag.

The 0.″2 resolved binary Aa,Ab is designated in the WDS as HDS 1850. Its preliminary orbit with a period of 31.6 yr determined by Tokovinin (2012) is updated here using recent speckle interferometry from SOAR and the RVs. So, the component A contains in fact three stars, all appearing in the CHIRON CCFs as distinct dips. The weak dip corresponding to Ab has not been detected with CORAVEL by Saar et al. (1990). Considering that B is now known to be an SB2, there are five stars in this multiple system. Several RVs of the components Aa1 and Aa2 measured with CHIRON are in excellent agreement with the SB2 orbit by Saar et al. (1990). There is no need to plot this circular orbit; its elements derived from the CHIRON data alone, with a fixed period, are listed in Table 3. Combining published and new data, the accurate period of 4.2334536 ± 0.0000018 days is determined. With a mass ratio is 0.998, the components of this twin binary are practically indistinguishable. Saar et al. (1990) estimated the orbital inclination as 85°, so there are no eclipses. The spectroscopic masses $M \sin^3 i$ of Aa1 and Aa2 are 1.085 $\mathcal{M}_\odot$.

The faint and close companion Ab has an average RV of 27.97 km s^{-1} with the rms scatter of 0.26 km s^{-1}. Its difference from the γ-velocity of Aa, 15.36 km s^{-1}, is caused by the motion in the 30-year orbit Aa,Ab. Using the RVs of Aa1 and Aa2 measured by Saar et al. (1990) with CORAVEL and here with CHIRON, I computed the RV of Aa (center of mass of the inner binary) as a weighted average, as explained in Paper I. Although the CORAVEL data cover a substantial time span from 1981.1 to 1989.2, only a minor RV change caused by the motion in the 30-yr orbit occurred during that time (Figure 8); naturally, no trend in the RV residuals of Aa1 and Aa2 has been noted so far.

New observations with CHIRON made 30 years later unfortunately fall on the same orbital phase, but contribute the RVs of Ab. The RV data, insufficient by themselves, are combined here with relative astrometry to update the orbit of Aa,Ab (Figure 8). It is seen almost exactly edge-on. I fixed the γ-velocity of Aa,Ab at 18.5 km s^{-1} to get the expected mass ratio of ∼1/3 and obtained the RV amplitudes of 3.93±0.23 and 11.06±0.34 km s^{-1} for Aa and Ab, respectively. As these spectroscopic elements of Aa,Ab are only a guess, they are not presented in Table 3.

Relative photometry of Aa,Ab at SOAR results in $\Delta y = 3.66$ mag, with a 0.06 mag rms scatter of the measures. As Aa1 and Aa2 are equal, the individual magnitudes of all three stars in the aggregate component A are estimated from the speckle photometry. The ratio of the CCF areas leads to $\Delta V_{\rm Aa,Ab} = 3.30$ mag, slightly underestimated because Ab is cooler than Aa1 and Aa2 and its lines are a bit stronger. The absolute magnitudes imply masses of about 1.2 and 0.7 $\mathcal{M}_\odot$ for Aa1 and Ab, respectively. However, the combined color index $V - K_s = 1.14$ mag estimated for three dwarf stars of such masses using the Dartmouth isochrone differs substantially from the actual color $V - K_s = 1.41$ mag. Apparently the components of the 4.3-day binary are larger and cooler than normal dwarfs.

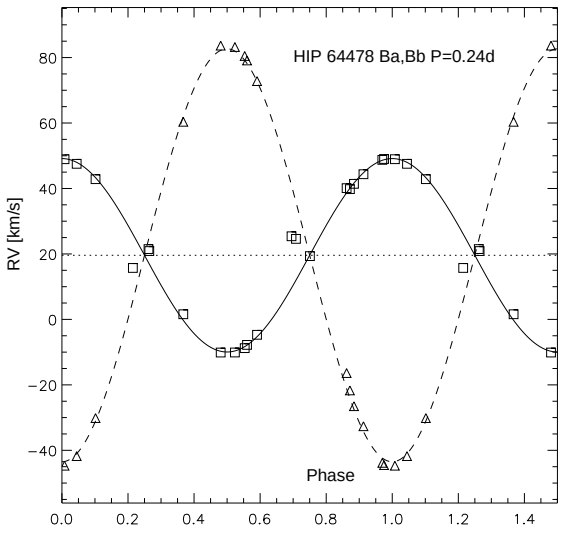

Figure 10. RV curve of the subsystem Ba,Bb with period 0.2435 days.

Spectroscopic observations of the component B with CHIRON in 2015 revealed it as a double-lined binary. Figure 9 shows three CCFs of B plotted on the same scale. The dips of Ba and Bb are obviously widened by the fast axial rotation. Gaussian fits to the CCFs are not very accurate. The stronger component Ba has a detail in its CCF that moves in anti-phase with Bb. The mean ratio of the areas of those Gaussians is 0.69, or $\Delta m = 0.40$ mag, for what it is worth.

The subsystem Ba,Bb has an unusually short period of 0.2435 days, found after several failed attempts to search for longer periods. Figure 10 shows the RV curve. Blended CCFs have not been used in the orbit fit, but these RVs are kept in the plot. The rms residuals to the circular orbit are rather large, 0.53 and 1.84 km s^{-1} for Ba and Bb, respectively.

The product $a\sigma$ is a measure of the CCF area. The sum of areas of Ba and Bb varies between 2.0 and 2.5 km s^{-1}, with an even lower value around 1.6 km s^{-1} measured on JD 2457121. Shallow CCFs correspond to the orbital phases when Ba is approaching and Bb is receding. Curiously, the spectrum of B has no Hα absorption line.

The subsystem Ba,Bb is a contact binary with a period of 5.8 hours, seen almost from the pole. Components of contact binaries are not normal dwarfs and do not follow standard relations. The secondary Bb is much brighter than follows from the mass ratio of 0.47. However, the complexity of an interacting binary means that the RVs measured here do not reflect the motion of the center of mass of each star.

The combined colors of B, $V - K_s = 2.73$ mag and $B - V = 1.17$ mag, correspond to a spectral type around K5V and imply individual masses of Ba and Bb of about 0.7 $\mathcal{M}_\odot$. The spectroscopic masses of Ba and Bb $M \sin^3 i$ are 0.013 and 0.006 $\mathcal{M}_\odot$. Assuming the mass of Ba to be 0.7 solar, the orbital inclination is ∼15°. The equa-

torial rotation speed of a solar-radius star synchronized with the orbit is $\sim$206 km s^{-1}, the projected rotational velocity is then $V \sin i \approx 52$ km s^{-1}. The stars apparently rotate synchronously with the orbit and fill their Roche lobes. The secondary is smaller and its projected rotation is 0.8 times less compared to the primary. The real mass ratio could be 0.8 or so. The quintuple system HIP 64478 bears some resemblance to the quintuple doubly-eclipsing system 1SWASP J093010.78+533859.5 containing low-mass close pairs with periods of 1.31 and 0.25 days (Lohr et al. 2015).

I looked in the ASAS database (Pojmanski 1997) to test whether the component B could be variable. Unfortunately, there are only a few measurements of B there. One night of photometric monitoring is needed to determine the amplitude or to set its upper limit.

8. DISCUSSION AND SUMMARY

This work started from monitoring secondary components of nearby solar-type stars in order to determine the frequency and parameters of subsystems. The new orbits given here strengthen statistical knowledge of low-mass binaries in the solar vicinity, reducing the number of subsystems with unknown periods. The primary components were measured as well for a consistency check and yielded interesting results, including the first orbit of HIP 28790 Aa,Ab, measurement of masses of HIP 12780 Aa,Ab, and the orbit of Aa,Ab in the three-tier hierarchy HIP 64478. In contrast, the subsystem Aa,Ab in HIP 9642 belongs to the primary component, while the faint and close visual secondary is not detected spectroscopically, making it a rather common and uninteresting triple.

Two secondary subsystems featured here are noteworthy. HIP 28790 Ba,Bb is an SB2 with a mass ratio of 0.89, yet very unequal components (Figure 6). There is no explanation of this paradox. This multiple system may be relatively young, as evidenced by its kinematics, the rotation of Aa, and the presence of lithium in its photosphere.

The binary HIP 64478 Ba,Bb is even more exotic, being a contact pair of 5.8 h period observed at low orbital inclination of $\sim$15°. This is probably a unique case, as other contact binaries are discovered photometrically by eclipses or by ellipsoidal variation. Contact binaries are relatively rare, about one per 500 stars of spectral types F, G, K (Rucinski 2002, 2006). Compared to the majority of known contact binaries, HIP 64478 Ba,Bb has a rather short period and a faint absolute magnitude of $M_V = 6.3$ mag. As its distance is well known, it can improve the currently known relation between period and absolute magnitude for contact systems. The sample of 4847 solar-type stars within 67 pc (Tokovinin 2014) contains 14 eclipsing systems with periods shorter than one day. The period of HIP 64478 Ba,Bb is the shortest in the whole sample. This bright, nearby, and unusually oriented system, if studied in greater detail, may provide interesting insights into physics of such merging pairs.

Looking at the mobile diagrams in Figure 1, we notice that when both visual components contain close subsystems, the period of the more massive primary is longer than the period of the secondary subsystem. Such a trend is expected from the general correlation between mass and angular momentum. It should be studied on a larger sample, as the evidence from only three cases is circumstantial.

Yet another feature of this diagram is a large ($\sim 10^3$) ratio of periods at the lowest hierarchical levels (i.e. a large vertical distance between the lowest and the next nodes). This could be a combined result of the formation process, where inner subsystems form first and shrink rapidly before acquiring outer companions, and the posterior dynamical evolution involving tidal friction and Kozai-Lidov cycles (Fabrycky & Tremaine 2007). This latter process works when inner pairs have separations of a few solar radii at periastron and the orbits have a large mutual inclination. It leaves a population of triples with inner periods of a few days and relative inclinations clustered around 39° and 141°. The inner binaries continue to interact tidally and their orbits are rapidly circularized. HIP 9642 Aa,Ab could result from such evolution, but not all inner subsystems match this scenario, being too wide and/or having eccentric orbits. So, tidal evolution cannot be a unique way to form close inner subsystems and some of them should be primordial. Considering large period ratios, formation of close subsystems by dynamical interactions in unstable small groups of nascent stars is unlikely, unless they evolved subsequently to much shorter periods.

I thank the operators of the 1.5-m telescope for executing observations of this program and the SMARTS team at Yale for scheduling and pipeline processing. Archival measures of resolved binaries were retrieved from the Washington database by B. Mason. I thank A.-M. Lagrange and S. Borgniet for communicating individual RVs of HIP 28790A, S. Rucinski for commenting upon the close binary HIP 64478 Ba,Bb and reading the paper draft. Referee's comments helped to improve the paper. This work used the SIMBAD service operated by Centre des Données Stellaires (Strasbourg, France), bibliographic references from the Astrophysics Data System maintained by SAO/NASA, the Washington Double Star Catalog maintained at USNO, and products of the 2MASS survey.

Facilities: CTIO:1.5m, SOAR

REFERENCES

Ammler-von Eiff, M. & Reiners, A. 2012, A&A, 542, 116
Cutispoto, G., Pastori, L., Pasquini, L. et al. 2002, A&A, 384, 491
Dotter, A., Chaboyer, B., Jevremović, D. et al. 2008, ApJS, 178, 89
Ehrenreich, D., Lagrange, A.-M., Montagnier, G. et al. 2010, A&A, 523, 73
Fabrycky D. & Tremaine S., 2007, ApJ, 669, 1298
Gray, R. O., Corbally, C. J., Garrison, R. F. et al. 2006, AJ, 132, 161
Hartkopf, W. I. & Mason, B. D. 2011, Inf. Circ., 175
Hartkopf, W. I., Tokovinin, A., & Mason, B. D. 2012, AJ, 143, 42
Kalas, P., Graham, J. R., Beckwith, S. V. W. et al. 2002, ApJ, 567, 999
Lagrange, A.-M., Desort, M., Galland, F. et al. 2009, A&A, 495, 335
Lohr, M. E., Norton, A. J., Gillen, E. et al. 2015, A&A, 578, 103.
Makarov, V. V. 2003, AJ, 126, 1966
Mannings, V. & Barlow, M. J. 1998, ApJ, 497, 330
Mason, B. D., Wycoff, G. L., Hartkopf, W. I., Douglass, G. G. & Worley, C. E. 2001, AJ, 122, 3466 (WDS)
Nordström, B., Mayor, M., Andersen, J. et al. 2004, A&A, 418, 989

Pojmanski, G., 1997, Acta Astronomica, 47, 467.
Rucinski, S. M. 2002, PASP, 114, 1124
Rucinski, S. M. 2006, MNRAS, 368, 1319
Saar, S. H., Nordström, B., & Andersen, J. 1990, A&A, 235, 291
Sylvester, R. J. & Mannings, V. 2000, MNRAS, 313, 73
Tokovinin, A., Hartung, M., & Hayward, T.L. 2010, AJ, 140, 510
Tokovinin, A., 2012, AJ, 144, 56
Tokovinin, A., Fischer, D. A., Bonati, M. et al. 2013, PASP, 125, 1336
Tokovinin, A. AJ, 2014, 147, 87
Tokovinin, A., Pribulla, T., & Fischer, D. 2015a, AJ, 149, 8
Tokovinin, A., Mason, B. D., Hartkopf, W. I. et al. 2015b, AJ, 150, 50
Tokovinin, A. 2015, AJ, 150, 177
Tokovinin, A. 2016, AJ, accepted (Paper I).
van Leeuwen, F. 2007, A&A, 474, 653 (HIP2)

Table 5
Radial velocities and residuals

HIP	System	Date (JD −2,400,000)	V_1	σ_1 (km s^{-1})	(O−C)$_1$	V_2	σ_2 (km s^{-1})	(O−C)$_2$	Ref.[a]
9642	Aa,Ab	54781.6711	36.080	0.500	0.290	64.320	0.500	0.273	L
9642	Aa,Ab	54782.5680	21.370	0.500	-0.254	79.860	0.500	-0.206	L
9642	Aa,Ab	56896.8724	41.060	0.200	0.029	58.201	0.200	0.080	C
9642	Aa,Ab	56938.8177	21.646	0.200	-0.140	79.949	0.200	0.066	C
9642	Aa,Ab	56967.5011	21.707	0.200	-0.111	79.893	0.200	0.046	C
9642	Aa,Ab	56969.6052	72.647	0.200	-0.100	22.373	0.200	0.117	C
9642	Aa,Ab	56977.6304	25.987	0.200	-0.031	75.204	0.200	0.106	C
9642	Aa,Ab	56978.7048	60.310	0.200	-0.093	36.206	0.200	-0.008	C
9642	Aa,Ab	56980.5951	55.197	0.200	-0.240	42.070	0.200	0.241	C
9642	Aa,Ab	56982.6278	31.182	0.200	-0.009	69.300	0.200	0.052	C
9642	Aa,Ab	56988.6238	70.384	0.200	-0.140	24.887	0.200	0.118	C
12780	Aa,Ab	55446.0506	0.235	10.000	-2.410	...	...	...	F
12780	Aa,Ab	56908.8456	-3.938	0.050	-0.161	2.846	0.050	-0.179	C
12780	Aa,Ab	56998.6952	-6.098	0.050	0.066	5.690	0.050	0.078	C
12780	Aa,Ab	57003.8085	-6.249	0.050	0.073	5.854	0.050	0.071	C
12780	Aa,Ab	57046.5419	-7.649	0.050	0.072	7.354	0.050	0.055	C
12780	Aa,Ab	57226.9715	-11.383	0.050	-0.066	11.150	0.050	-0.046	C
12780	Aa,Ab	57226.9715	-11.400	0.050	-0.083	11.119	0.050	-0.077	C
12780	Aa,Ab	57319.7430	-7.905	0.050	0.110	7.705	0.050	0.088	C
12780	Ba,Bb	55445.8833	-10.646	2.000	-0.016	...	...	...	F
12780	Ba,Bb	56908.8883	16.010	0.200	-0.003	...	...	...	C
12780	Ba,Bb	56937.6987	18.094	0.200	0.009	...	...	...	C
12780	Ba,Bb	56998.6192	6.252	0.200	-0.002	...	...	...	C
12780	Ba,Bb	57003.7136	-19.018	0.200	-0.003	...	...	...	C
12780	Ba,Bb	57008.6948	-12.497	0.200	-0.001	...	...	...	C
12780	Ba,Bb	57009.6803	-10.238	0.200	-0.003	...	...	...	C
12780	Ba,Bb	57046.5915	13.321	0.200	-0.010	...	...	...	C
12780	Ba,Bb	57226.9011	-18.911	0.200	0.003	...	...	...	C
12780	Ba,Bb	57319.6545	1.207	0.200	0.008	...	...	...	C
12780	Ba,Bb	57333.6777	-7.920	0.200	0.002	...	...	...	C
28790	Aa,Ab	53989.8028	30.368	0.100	0.016	...	...	...	H
28790	Aa,Ab	53989.8067	30.357	0.100	0.005	...	...	...	H
28790	Aa,Ab	54056.8309	28.500	0.100	-0.020	...	...	...	H
28790	Aa,Ab	54056.8348	28.494	0.100	-0.026	...	...	...	H
28790	Aa,Ab	54057.7883	28.421	0.100	-0.054	...	...	...	H
28790	Aa,Ab	54057.7924	28.420	0.100	-0.055	...	...	...	H
28790	Aa,Ab	54386.7594	29.790	0.100	0.019	...	...	...	H
28790	Aa,Ab	54386.7650	29.798	0.100	0.026	...	...	...	H
28790	Aa,Ab	54389.8641	30.022	0.100	0.054	...	...	...	H
28790	Aa,Ab	54389.8749	30.022	0.100	0.053	...	...	...	H
28790	Aa,Ab	54392.8366	30.125	0.100	0.014	...	...	...	H
28790	Aa,Ab	54392.8416	30.125	0.100	0.013	...	...	...	H
28790	Aa,Ab	54393.7776	30.151	0.100	0.002	...	...	...	H
28790	Aa,Ab	54393.7829	30.155	0.100	0.006	...	...	...	H
28790	Aa,Ab	54394.7703	30.213	0.100	0.027	...	...	...	H
28790	Aa,Ab	54394.7754	30.220	0.100	0.034	...	...	...	H
28790	Aa,Ab	54422.7526	30.445	0.100	0.002	...	...	...	H
28790	Aa,Ab	54425.8466	30.432	0.100	0.012	...	...	...	H
28790	Aa,Ab	54428.7658	30.384	0.100	-0.010	...	...	...	H
28790	Aa,Ab	54452.7270	30.008	0.100	-0.009	...	...	...	H
28790	Aa,Ab	54485.5476	29.080	0.100	-0.017	...	...	...	H
28790	Aa,Ab	54521.5978	27.177	0.100	-0.044	...	...	...	H
28790	Aa,Ab	54542.5150	24.958	0.100	-0.046	...	...	...	H
28790	Aa,Ab	54558.5899	21.228	0.100	0.039	...	...	...	H
28790	Aa,Ab	54558.5937	21.212	0.100	0.025	...	...	...	H
28790	Aa,Ab	54781.8038	20.280	0.500	-0.156	...	...	...	L
28790	Aa,Ab	56961.8068	26.872	0.100	0.053	...	...	...	C
28790	Aa,Ab	56996.7491	19.937	0.100	0.011	...	...	...	C
28790	Aa,Ab	56997.7431	19.427	0.100	0.012	...	...	...	C
28790	Aa,Ab	56998.7520	18.917	0.100	0.074	...	...	...	C
28790	Aa,Ab	57003.7703	14.719	0.100	-0.030	...	...	...	C
28790	Aa,Ab	57008.7167	5.810	0.100	-0.058	...	...	...	C
28790	Aa,Ab	57009.7352	2.627	0.100	0.032	...	...	...	C
28790	Aa,Ab	57027.6661	26.845	0.100	-0.013	...	...	...	C
28790	Aa,Ab	57040.7020	29.458	0.100	-0.092	...	...	...	C
28790	Aa,Ab	57261.9109	29.440	0.100	-0.094	...	...	...	C
28790	Aa,Ab	57319.6913	30.265	0.100	0.043	...	...	...	C
28790	Aa,Ab	57332.7685	29.977	0.100	0.003	...	...	...	C
28790	Ba,Bb	54781.8075	17.960	0.500	-0.291	39.520	0.500	-0.223	L
28790	Ba,Bb	56934.8785	46.794	0.500	-0.266	...	...	...	C
28790	Ba,Bb	56937.7719	29.357	0.500	0.475	...	...	...	C
28790	Ba,Bb	56961.8014	47.172	0.500	0.142	7.109	0.500	-0.326	C
28790	Ba,Bb	56996.7440	28.044	0.500	0.163	...	...	...	C
28790	Ba,Bb	56997.7384	33.856	0.500	-0.516	...	...	...	C

Table 5 — *Continued*

HIP	System	Date (JD −2,400,000)	V_1	σ_1 (km s^{-1})	(O−C)$_1$	V_2	σ_2 (km s^{-1})	(O−C)$_2$	Ref.[a]
28790	Ba,Bb	56998.7472	40.022	0.500	0.096	16.304	5.000	0.894	C
28790	Ba,Bb	57003.7650	31.066	0.500	-0.177	...	...	...	C
28790	Ba,Bb	57008.7114	18.755	0.500	0.270	42.106	5.000	2.625	C
28790	Ba,Bb	57009.7300	26.368	0.500	0.222	...	...	...	C
28790	Ba,Bb	57027.6764	47.290	0.500	0.158	7.304	0.500	-0.017	C
28790	Ba,Bb	57040.7063	47.273	0.500	0.227	7.051	0.500	-0.366	C
28790	Ba,Bb	57261.9131	30.987	1.000	-0.605	...	...	...	C
28790	Ba,Bb	57319.7004	45.449	0.500	-0.075	9.773	0.500	0.647	C
28790	Ba,Bb	57332.7705	46.043	0.500	-0.032	8.514	1.000	0.006	C
64478	Aa1,Aa2	57141.6159	100.176	1.000	0.037	-69.700	1.000	-0.177	C
64478	Aa1,Aa2	57162.5490	92.760	1.000	-0.129	-61.948	1.000	0.301	C
64478	Aa1,Aa2	57162.6056	95.449	1.000	-0.094	-64.623	1.000	0.289	C
64478	Aa1,Aa2	57166.5739	78.058	1.000	-0.527	-47.751	1.000	0.146	C
64478	Aa1,Aa2	57166.5760	78.336	1.000	-0.426	-47.946	1.000	0.128	C
64478	Aa1,Aa2	57169.5730	-56.343	1.000	-0.610	87.491	1.000	0.612	C
64478	Aa1,Aa2	57170.5171	47.611	1.000	-1.484	-17.454	1.000	0.852	C
64478	Aa1,Aa2	57175.6150	100.178	1.000	0.402	-69.357	1.000	-0.198	C
64478	Aa1,Aa2	57177.4994	-67.318	1.000	0.013	98.407	1.000	-0.109	C
64478	Aa1,Aa2	57177.6185	-69.709	1.000	-0.331	100.414	1.000	-0.156	C
64478	Aa,Ab	44646.5692	15.717	0.500	-0.178	...	...	...	S
64478	Aa,Ab	45016.9248	16.026	0.500	0.301	...	...	...	S
64478	Aa,Ab	46142.9665	15.470	0.500	0.089	...	...	...	S
64478	Aa,Ab	47189.7507	15.248	0.500	-0.122	...	...	...	S
64478	Aa,Ab	47190.8464	15.416	0.500	0.046	...	...	...	S
64478	Aa,Ab	47191.9421	16.380	0.500	1.010	...	...	...	S
64478	Aa,Ab	47193.0378	15.322	0.500	-0.049	...	...	...	S
64478	Aa,Ab	47193.7683	14.742	0.500	-0.629	...	...	...	S
64478	Aa,Ab	47194.8641	16.326	0.500	0.955	...	...	...	S
64478	Aa,Ab	47220.7962	14.576	0.500	-0.800	...	...	...	S
64478	Aa,Ab	47221.8920	14.500	0.500	-0.876	...	...	...	S
64478	Aa,Ab	47545.8618	15.987	0.500	0.527	...	...	...	S
64478	Aa,Ab	47546.9575	15.082	0.500	-0.378	...	...	...	S
64478	Aa,Ab	47547.6880	15.397	0.500	-0.063	...	...	...	S
64478	Aa,Ab	47548.7837	16.128	0.500	0.667	...	...	...	S
64478	Aa,Ab	47549.8795	15.479	0.500	0.018	...	...	...	S
64478	Aa,Ab	47602.8396	15.241	0.500	-0.238	...	...	...	S
64478	Aa,Ab	47603.9353	15.383	0.500	-0.097	...	...	...	S
64478	Aa,Ab	47604.6658	14.991	0.500	-0.489	...	...	...	S
64478	Aa,Ab	47605.7615	15.316	0.500	-0.165	...	...	...	S
64478	Aa,Ab	47606.8573	15.291	0.500	-0.190	...	...	...	S
64478	Aa,Ab	47607.9530	15.433	0.500	-0.048	...	...	...	S
64478	Aa,Ab	47608.6835	15.494	0.500	0.012	...	...	...	S
64478	Aa,Ab	47609.7792	16.075	0.500	0.593	...	...	...	S
64478	Aa,Ab	57162.6889	...	...	...	28.004	0.250	0.039	C
64478	Aa,Ab	57162.6889	...	...	...	27.628	0.250	-0.337	C
64478	Aa,Ab	57166.7066	...	...	...	27.987	0.250	0.021	C
64478	Aa,Ab	57166.7066	...	...	...	28.273	0.250	0.307	C
64478	Aa,Ab	57169.2633	15.360	0.200	0.029	28.413	0.250	0.446	C
64478	Aa,Ab	57175.4724	...	...	...	27.892	0.250	-0.077	C
64478	Aa,Ab	57177.6638	...	...	...	27.944	0.250	-0.025	C
64478	Aa,Ab	57177.6638	...	...	...	27.627	0.250	-0.342	C
64478	Ba,Bb	57040.8218	48.951	0.500	-0.145	-44.695	2.000	-1.286	C
64478	Ba,Bb	57078.7886	44.359	0.500	-0.445	-32.636	2.000	1.609	C
64478	Ba,Bb	57093.7293	20.882	20.000	3.968	...	...	...	C
64478	Ba,Bb	57098.7453	40.107	0.500	1.422	-16.396	2.000	4.786	C
64478	Ba,Bb	57120.6680	41.426	0.500	-0.206	-26.514	2.000	0.958	C
64478	Ba,Bb	57121.7598	1.572	20.000	1.846	60.377	2.000	-1.617	C
64478	Ba,Bb	57125.5607	49.006	0.500	0.232	-44.507	2.000	-1.786	C
64478	Ba,Bb	57130.5543	-10.122	20.000	-0.385	83.650	20.000	1.453	C
64478	Ba,Bb	57131.5839	24.598	20.000	12.628	...	...	...	C
64478	Ba,Bb	57134.6295	15.717	20.000	-10.357	...	...	...	C
64478	Ba,Bb	57137.7357	48.745	0.500	0.138	-43.823	2.000	-1.459	C
64478	Ba,Bb	57141.6503	47.531	0.500	-0.449	-41.768	2.000	-0.742	C
64478	Ba,Bb	57162.5514	39.797	0.500	-0.251	-21.691	2.000	2.401	C
64478	Ba,Bb	57162.6074	42.843	0.500	-0.461	-30.154	2.000	0.888	C
64478	Ba,Bb	57169.5361	-8.785	0.500	-0.472	80.482	2.000	1.326	C
64478	Ba,Bb	57169.5378	-7.794	0.500	0.066	79.113	2.000	0.924	C
64478	Ba,Bb	57169.5706	25.404	20.000	15.822	...	...	...	C
64478	Ba,Bb	57170.5193	-4.710	0.500	0.577	72.806	2.000	0.109	C
64478	Ba,Bb	57175.6170	-10.108	0.500	-0.476	83.218	2.000	1.246	C
64478	Ba,Bb	57177.5015	21.481	10.000	4.122	...	...	...	C
64478	Ba,Bb	57177.6205	19.332	10.000	-0.382	...	...	...	C

[a] C: CHIRON; F: FECH; S: Saar et al. (1990); H: HARPS; L: Tokovinin (2015).

Table 6
Position measurements and residuals

HIP	System	Date (yr)	θ (°)	ρ ($''$)	σ ($''$)	$(O-C)_\theta$ (°)	$(O-C)_\rho$ ($''$)	Ref.[a]
9642	A,B	1932.9100	177.9	1.020	0.500	34.9	-0.196	Vis
9642	A,B	1935.6600	159.6	1.170	0.050	13.1	-0.042	Vis
9642	A,B	1936.9500	153.8	0.960	0.200	5.7	-0.251	Vis
9642	A,B	1956.8600	165.9	0.960	0.200	-8.0	-0.233	Vis
9642	A,B	1991.2500	218.0	1.332	0.010	1.6	0.030	HIP
9642	A,B	2008.5407	233.7	1.425	0.002	-0.1	-0.004	Spe
9642	A,B	2008.7700	233.9	1.427	0.002	-0.1	-0.004	SOAR
9642	A,B	2011.0393	236.0	1.448	0.002	0.0	-0.002	SOAR
9642	A,B	2011.0393	236.1	1.448	0.002	0.0	-0.002	SOAR
9642	A,B	2012.9205	237.6	1.463	0.002	-0.1	-0.002	SOAR
9642	A,B	2012.9205	237.6	1.462	0.002	-0.1	-0.004	SOAR
9642	A,B	2012.9205	237.6	1.463	0.002	-0.1	-0.002	SOAR
9642	A,B	2015.0284	239.6	1.488	0.002	0.1	0.005	SOAR
9642	A,B	2015.0284	239.6	1.487	0.002	0.1	0.003	SOAR
9642	A,B	2015.1050	239.4	1.490	0.002	-0.1	0.006	SOAR
9642	A,B	2015.7383	240.3	1.494	0.002	0.2	0.005	SOAR
9642	A,B	2015.9131	240.3	1.490	0.002	0.1	-0.001	SOAR
12780	Aa,Ab	1963.0500	142.7	0.1140	1.0500	3.5	0.0324	Fin
12780	Aa,Ab	1964.0340	171.4	0.1400	0.0500	1.5	0.0097	Fin
12780	Aa,Ab	1965.0460	185.4	0.1380	0.0500	-1.9	-0.0109	Fin
12780	Aa,Ab	1966.0200	173.1	0.1400	1.0500	-30.1	0.0009	Vis
12780	Aa,Ab	1966.0620	209.1	0.1280	0.0500	5.2	-0.0101	Fin
12780	Aa,Ab	1967.1530	230.2	0.1290	0.0500	-0.9	0.0320	Fin
12780	Aa,Ab	1978.9700	193.1	0.1700	0.0500	-2.7	0.0233	Vis
12780	Aa,Ab	1989.9330	146.0	0.0890	0.0020	1.5	0.0007	Spe
12780	Aa,Ab	1990.9130	172.5	0.1340	0.0020	0.4	0.0004	Spe
12780	Aa,Ab	1990.9240	172.8	0.1340	0.0020	0.5	0.0000	Spe
12780	Aa,Ab	1991.7210	184.2	0.1460	0.0020	-1.7	-0.0024	Spe
12780	Aa,Ab	1991.7240	186.1	0.1490	0.0020	0.2	0.0006	Spe
12780	Aa,Ab	2008.6060	339.1	0.0510	0.0020	-1.3	-0.0004	SOAR
12780	Aa,Ab	2008.6060	339.2	0.0510	0.0020	-1.2	-0.0004	SOAR
12780	Aa,Ab	2009.6710	122.2	0.0650	0.0020	-2.3	-0.0019	SOAR
12780	Aa,Ab	2009.7560	130.1	0.0730	0.0020	-0.5	0.0008	SOAR
12780	Aa,Ab	2010.9660	171.8	0.1340	0.0020	0.2	0.0012	SOAR
12780	Aa,Ab	2013.7480	223.0	0.1100	0.0020	0.2	0.0008	SOAR
12780	Aa,Ab	2014.7690	279.1	0.0620	0.0020	1.8	0.0017	SOAR
12780	Aa,Ab	2014.7690	280.9	0.0600	0.0020	3.6	-0.0003	SOAR
12780	Aa,Ab	2015.0280	304.4	0.0520	0.0020	-1.3	-0.0014	SOAR
64478	Aa,Ab	1991.2500	96.0	0.1870	0.0100	-5.0	-0.0015	HIP
64478	Aa,Ab	2001.0820	277.1	0.2420	0.0050	-3.3	-0.0021	Spe
64478	Aa,Ab	2011.0400	98.8	0.2760	0.0020	-0.1	-0.0024	SOAR
64478	Aa,Ab	2011.0400	98.4	0.2790	0.0020	-0.5	0.0006	SOAR
64478	Aa,Ab	2012.1020	99.2	0.3160	0.0020	0.1	0.0018	SOAR
64478	Aa,Ab	2014.3010	99.6	0.3560	0.0020	0.1	0.0014	SOAR
64478	Aa,Ab	2015.2500	99.9	0.3550	0.0020	0.3	-0.0009	SOAR
64478	Aa,Ab	2015.2500	99.8	0.3560	0.0020	0.2	0.0001	SOAR

[a] Fin: ocular interferometry by W. S. Finsen; HIP: Hipparcos; SOAR: speckle interferometry at SOAR; Spe: speckle interferometry at other telescopes; Vis: visual micrometer measures.